Verification of Knoop indenters with Gal-Indent optical system

A. Prato, C. Origlia, A. Germak

Verification of Knoop indenters with Gal-Indent optical system

T.R. 8/2020 March 2020

I.N.RI.M. TECHNICAL REPORT

Abstract in Italiano

Le normative internazionali ISO 4545-2 e 4545-3 per i test di durezza Knoop richiedono la verifica geometrica dei penetratori. Il laboratorio di durezza INRiM, in collaborazione con la Galileo-LTF®, ha sviluppato uno specifico sistema ottico di misurazione(commercializzato da Galileo-LTF® come Gal-Indent) , utilizzato per la verifica dei penetratori Vickers. Questo sistema è in grado di misurare i due angoli al vertice tra due facce opposte, i quattro angoli della base quadrangolare e l'angolo tra l'asse della piramide di diamante e l'asse del codolo del penetratore. Usando le misure degli angoli al vertice e della base come input di un appropriato modello geometrico, gli angoli al vertice tra spigoli opposti di penetratori Knoop, nominalmente di 172.5° e 130°, e l'angolo tra l'asse della piramide di diamante e l'asse del supporto del penetratore, nominalmente di 0°, possono essere verificati con un'incertezza estesa di 0.05°, come richiesto dalle normative. Il confronto tra le misure sperimentali eseguite con questo metodo su tre diversi penetratori Knoop, precedentemente verificati da un laboratorio accreditato tedesco, mostrano risultati compatibili, in termini di errore normalizzato.

Abstract in Inglese

ISO 4545-2 and 4545-3 of Knoop hardness tests require the geometrical verification of the indenters. INRiM hardness laboratory, in cooperation with Galileo-LTF® has developed a specific optical measuring system (commercialized by Galileo-LTF® as Gal-Indent) which is addressed for the verification of Vickers indenters. This system is able to measure the two vertex angles between two opposite faces, the four angles of the quadrilateral base and the angle between the axis of the diamond pyramid and the axis of the indenter holder. Using the measured quantities of the vertex and base angles as inputs of a suitable geometrical model, the angles from the opposite edges at the vertex of Knoop indenters, nominally 172.5° and 130°, and the angle between the axis of the diamond pyramid and the axis of the indenter holder, nominally 0°, can be verified with an expanded uncertainty of 0.05°, as required by the relevant Standard. Comparison of experimental measurements performed on three different Knoop indenters, previously verified by a German accredited laboratory, shows compatible results in terms of normalized error.

Contents

1 Introduction

Knoop indenter is a rhombic-based pyramidal diamond that produces an elongated diamond-shaped indent. The angles from the opposite edges at the vertex of the diamond pyramid of the indenter, α and β, are 172.5° and 130°, respectively, and the ratio between long and short diagonals is approximately 7.11 to 1 (Fig. 1). This entails that the angles of the rhombic base, φ_i and τ_i (i=1,2), are approximately 164° and 16°, respectively, and that the angles between the two opposite faces of the vertex θ are approximately 129.57°. ISO 4545-2 and 4545-3 [1,2] specify the requirements of the indenters with different tolerances. The second is more restrictive since it refers to the calibration of reference blocks. The tolerance for the angle of 172.5° is ±0.1° in both documents, whereas for 130° the tolerance is ±1° and ±0.1°, respectively. Furthermore, the angle δ between the axis of the diamond pyramid and the axis of the indenter holder (normal to the seating surface), named tilt angle, shall not exceed 0.5° and 0.3°, respectively. The four faces of the diamond pyramid shall also be polished and free from surface defects and the indenter constant c=tan(β/2)/(2tan(α/2)) shall be within 1,0 % of the ideal value 0.07028. In addition, the device used for the verification shall have a maximum expanded uncertainty of 0.07°. Currently, INRiM hardness laboratory in cooperation with Galileo-LTF® [3,4], has developed a specific optical measuring system (com-mercialized by the Galileo-LTF® as Gal-Indent) for the verification of the geometrical characteristics of Vickers indenters [5]. This system is able to directly measure the main geometrical parameters of Vickers indenters required by the standard, i.e. the two vertex angles (nominally 136°) between two opposite faces and the four angles of the square base, both with an expanded uncertainty of 0.05°. By measuring these quantities and with a suitable geometrical model, it is possible to evaluate the standard geometrical parameters required by Knoop standards.

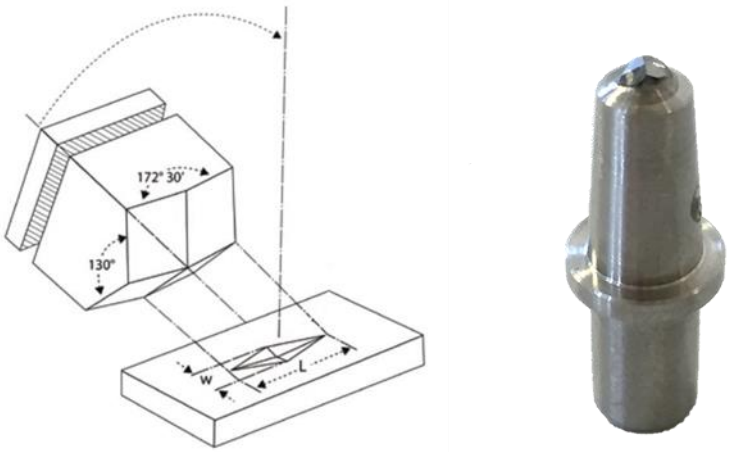

Fig. 1 - Schematic draw (left) and picture (right) of a typical Knoop indenter.

2 The Gal-Indent optical system

In INRiM hardness laboratory a specific measuring system, commercialized by Galileo-LTF® as Gal-Indent optical system (Fig. 2), was developed and is currently used for the verification of Vickers indenters. The system is also adopted by different National Metrological Institutes (NMIs) and calibration laboratories around the world. It is able to measure the two vertex angles of the indenter between two opposite faces, and the four angles between two consecutive faces by means of two angular encoders mounted on the optical measuring system [6].

The optical system is based on Mirau interferometry, where a 546 nm light beam is split into two beams: one is reflected to the observer through the eyepieces, the other hits a Vickers indenter lateral face and is reflected back to the observer, thus generating an interference pattern. The indenter is simultaneously rotated around the axis, passing through the pyramid vertex, normal to the plane containing the indenter-holder axis and the optical lens axis, and around the indenter-holder axis, until a lateral face is parallel to the plane of the microscope lens by observing the interference fringes. These two rotations are measured by means of two angular encoders. Rotations around the indenter-holder axis represent the measurement of the angles between two consecutive faces, i.e. the quadrilateral base angles; whereas, rotations around the axis normal to the plane containing the indenter-holder axis and the optical lens axis represent the measurement of the supplementary angles for each lateral face from which the angles between two opposite faces are easily obtained [7], as required for the verification of Vickers indenters. Using these measurements as input of a suitable geometrical model, presented in the following Section, the possibility to evaluate the geometrical parameters of Knoop indenters is investigated.

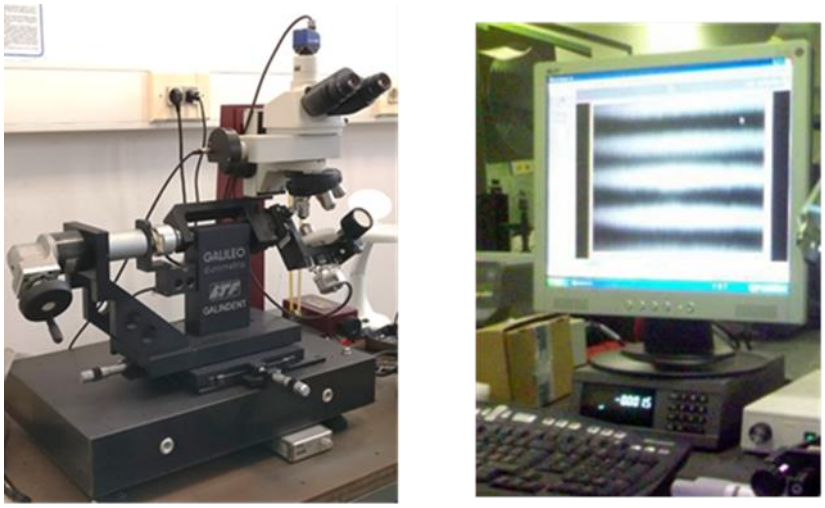

Fig. 2 - The Galileo-LTF® Gal-Indent optical system used at INRiM hardness laboratory for the measurement of the vertex angles and the quadrilateral base angles.

3. The geometrical model

3.1 Evaluation of the tilt angle

The geometry of an ideal Knoop indenter, i.e. an indenter with four generic faces (A, B, C, D), with angles from the opposite edges at the vertex of the diamond pyramid α and β equal to 172.5° and 130°, respectively, with angles θ between two opposite faces equal to 129.57°, and with a tilt angle δ equal to 0°, is schematically depicted in Fig. 3. *xyz* and *x′y′z′* coordinate systems correspond, respectively, to the diagonals of the Knoop indenter rhombic base, and to the optical reference system that is perpendicular to the perimeter of two opposite faces. Therefore, the angle between *x*- and *y*-axis is nominally 90°, whereas the angle σ_{AB} between *x′*- and *y′*-axis is nominally 164°. For each *j*-th face (*j* = A, B, C, D), the intersection between an optical reference axis (*x′*- or *y′*-axis) and the base perimeter is identified by point H_j, whereas the intersection with *x*- and *y*-axis are identified by points S_j and P_j, respectively (thus $S_A \equiv S_D$, $S_B \equiv S_C$, $P_A \equiv P_B$, $P_C \equiv P_D$). The pyramid vertex V is arbitrarily placed on $z = 1$. A cross-section of an ideal Knoop indenter along *x′z′* optical system plane is also shown in Fig. 4. The quadrilateral base angles φ_i and τ_i (i = 1,2), nominally 164° and 16°, respectively, and the supplementary angles of each *j*-

th lateral face (A, B, C, D) along x' and y'-axis, ω_j, nominally (180°-129.57°) / 2 ≈ 25.22°, are measured by means of the optical system previously described.

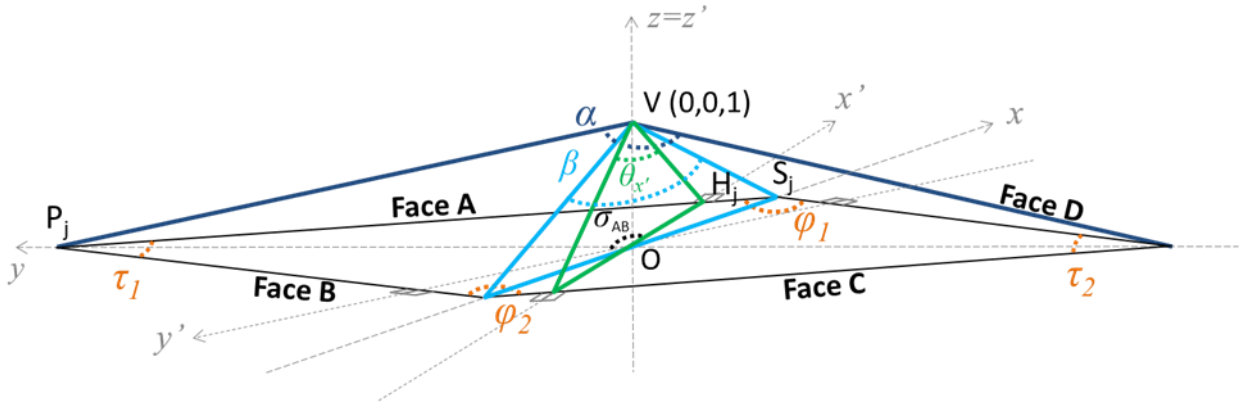

Fig. 3 - 3-D schematic representation of an ideal Knoop indenter rhombic-based pyramid

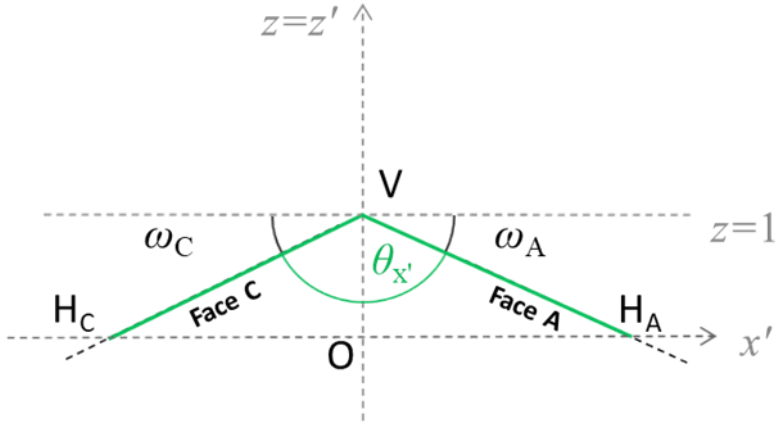

Fig. 4 - Cross-section of an ideal Knoop indenter along x'z' optical reference system plane

However, in real Knoop indenters, the tilt angle δ between the axis of the diamond pyramid $\mathbf{v} = \overrightarrow{OV} = (v_x,v_y,v_z)$ and the axis of the indenter holder angle (z'-axis) is not exactly 0°, thus an angle γ between the projection of the pyramid vertex on $z = 0$ plane and x'-axis appears, as shown in Fig. 5.

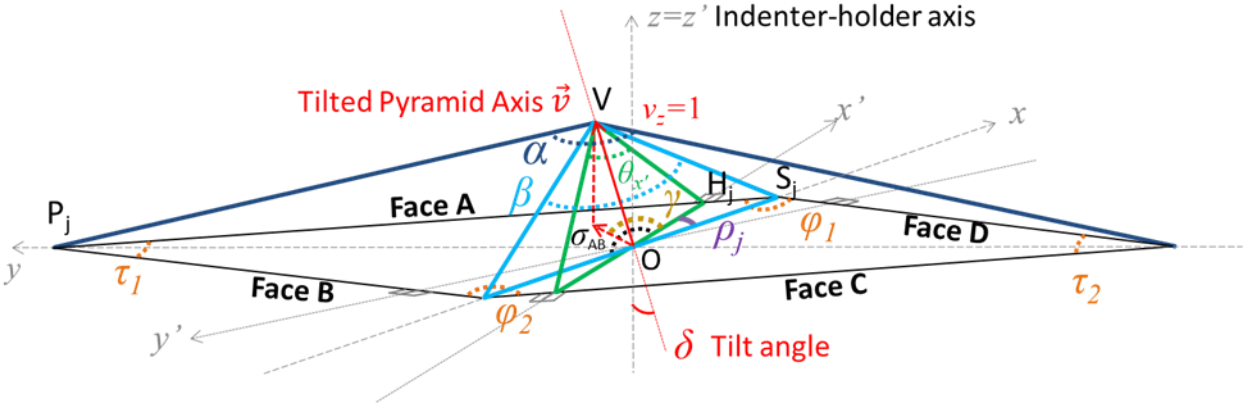

Fig. 5 - 3-D schematic representation of a real Knoop indenter rhombic-based pyramid

From quadrilateral base angles measurements φ_i and τ_i (i = 1,2), in order to take into account possible asymmetries of the rhombic-base, the mean angle $\rho_j = \widehat{H_jOS_j}$ between xy and $x'y'$ reference systems (e.g., in Fig. 5 for face A between x'- and x-axis), for each j-th indenter face, can be evaluated according to

$$\rho_j = \frac{\left(90 - \frac{\varphi_j}{2}\right) + \frac{\tau_j}{2}}{2} \tag{1}$$

where $\varphi_A = \varphi_D = \varphi_1$, $\varphi_B = \varphi_C = \varphi_2$, $\tau_A = \tau_B = \tau_1$, $\tau_C = \tau_D = \tau_2$.

In this way, considering the mean value $\rho = \sum_{j=1}^{4} \rho_j/4$ among the four faces, the angle σ_{AB} between x'- and y'-axis can be obtained according to Eq. (2).

$$\sigma_{AB} = 180 - 2\rho \tag{2}$$

From the measurement of the supplementary angles ω_j of each j-th lateral face, the two vertex angles $\theta_{x'}$ and $\theta_{y'}$ and the pyramid tilt angles $\delta_{x'}$ and $\delta_{y'}$, along x'- and y'- axis, can be calculated according to Eqs. (3) and (4), respectively. By way of example, in Fig. 6, the cross-section of a real Knoop indenter through $x'z'$ plane shows the measured vertex angle $\theta_{x'}$ and the pyramid tilt angle $\delta_{x'}$.

$$\theta_{x'} = 180 - (\omega_A + \omega_C); \qquad \theta_{y'} = 180 - (\omega_B + \omega_D) \tag{3}$$

$$\delta_{x'} = \frac{\omega_A - \omega_C}{2}; \quad \delta_{y'} = \frac{\omega_B - \omega_D}{2} \tag{4}$$

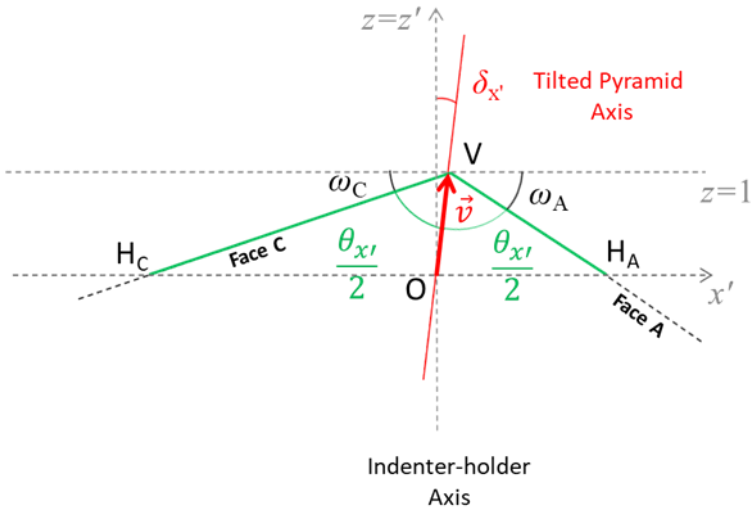

Fig. 6 - Cross-section of a real Knoop indenter along x'z' optical reference system plane

By decomposing the pyramid tilted axis vector **v** along non-orthogonal *x'z'* and *y'z'* planes, according to Fig. 7 and Fig. 8, Eq. (5) is derived. Successively, implementing the equations of non-orthogonal systems (Fig. 9) and using Eq. (5), Eqs. (6)-(8) and Eqs. (9)-(10) can be derived.

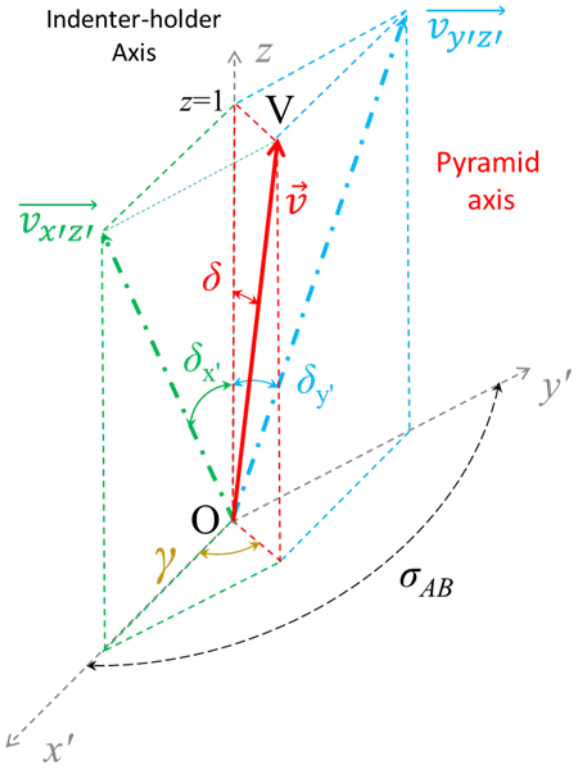

Fig. 7 - Decomposition of the tilted pyramid axis vector v and the associated angles along x'- and y'- axis

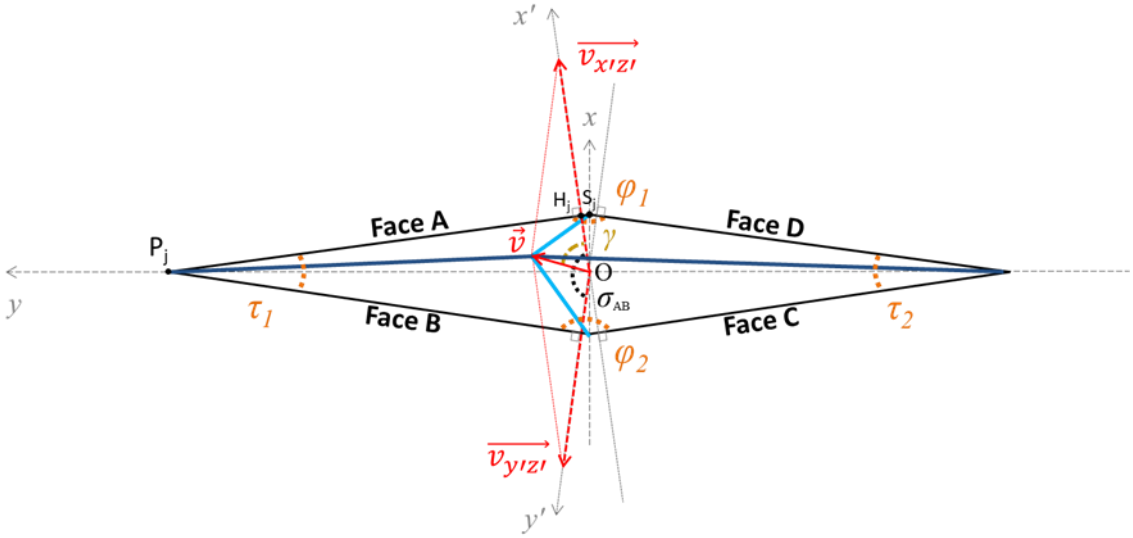

Fig. 8 - Upper view of a real Knoop indenter with tilted pyramid axis vector v and the associated projections along x'- and y'- axis

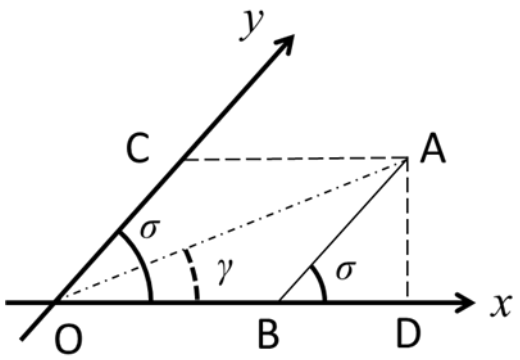

$$\begin{cases} \overline{OA}\cos\gamma = \overline{OB} + \overline{OC}\cos\sigma \\ \overline{OA}\sin\gamma = \overline{OC}\sin\sigma \end{cases}$$

Fig. 9 - Generic non-orthogonal reference system with relevant equations

$$\|\mathbf{v}\|\cos\delta = \|\mathbf{v}_{x'z'}\|\cos\delta_{x'} = \left\|\mathbf{v}_{y'z'}\right\|\cos\delta_{y'} \tag{5}$$

$$\|\mathbf{v}\|\sin\delta\cos\gamma = \|\mathbf{v}_{x'z'}\|\ \sin\delta_{x'} + \left\|\mathbf{v}_{y'z'}\right\|\ \sin\delta_{y'}\cos\sigma_{AB} = \|\mathbf{v}\|\ \frac{\cos\delta}{\cos\delta_{x'}}\ \sin\delta_{x'} + \|\mathbf{v}\|\ \frac{\cos\delta}{\cos\delta_{y'}}\ \sin\delta_{y'}\cos\sigma_{AB} \tag{6}$$

$$\sin\delta\cos\gamma = \frac{\cos\delta}{\cos\delta_{x'}}\ \sin\delta_{x'} + \frac{\cos\delta}{\cos\delta_{y'}}\ \sin\delta_{y'}\cos\sigma_{AB} \tag{7}$$

$$\tan\delta\cos\gamma = \tan\delta_{x'} + \tan\delta_{y'}\cos\sigma_{AB} \tag{8}$$

$$\|\mathbf{v}\|\sin\delta\sin\gamma = \left\|\mathbf{v}_{y'z'}\right\|\ \sin\delta_{y'}\sin\sigma_{AB} = \|\mathbf{v}\|\ \frac{\cos\delta}{\cos\delta_{y'}}\sin\delta_{y'}\sin\sigma_{AB} \tag{9}$$

$$\tan\delta\sin\gamma = \tan\delta_{y'}\sin\sigma_{AB} \tag{10}$$

By performing the squared sum of Eqs. (8) and (10), the total tilt angle δ can be obtained (see Eqs. (11)-(13)):

$$\tan^2\delta\cos^2\gamma + \tan^2\delta\sin^2\gamma = \tan^2\delta_{x'} + \tan^2\delta_{y'}\cos^2\sigma_{AB} + 2\tan\delta_{x'}\tan\delta_{y'}\cos\sigma_{AB} + \tan^2\delta_{y'}\sin^2\sigma_{AB} \tag{11}$$

$$\tan^2\delta = \tan^2\delta_{x'} + \tan^2\delta_{y'} + 2\tan\delta_{x'}\tan\delta_{y'}\cos\sigma_{AB} \tag{12}$$

$$\delta = \arctan\sqrt{\tan^2\delta_{x'} + \tan^2\delta_{y'} + 2\ \tan\delta_{x'}\ \tan\delta_{y'}\cos(\sigma_{AB})} \tag{13}$$

By performing the ratio between Eqs. (10) and (8), the angle γ can be derived (see Eqs. (14)-(15)):

$$\tan\gamma = \frac{\tan\delta_{y'}\sin\sigma_{AB}}{\tan\delta_{x'} + \tan\delta_{y'}\cos\sigma_{AB}} \tag{14}$$

$$\gamma = \arctan\left(\frac{\tan\delta_{y'}\sin\sigma_{AB}}{\tan\delta_{x'} + \tan\delta_{y'}\cos\sigma_{AB}}\right) \tag{15}$$

3.1 Evaluation of the angles between the opposite edges at the vertex

From the scheme of Fig. 5 and reminding that the pyramid vertex V is placed on $z = 1$, the vector of the tilted pyramid axis **v** referred to the *xyz* reference system can be written according to Eq. (16), where ρ is the mean angle between x'- and x-axis (see Eq. (2)).

$$\mathbf{v} = [\tan(\delta)\cos(\gamma+\rho), \tan(\delta)\sin(\gamma+\rho), 1] \tag{16}$$

Considering the triangle OH_jV in Fig. 5 and Fig. 6 for each j-th indenter face (A, B, C, D), given that $\widehat{OH_jV} = \omega_j$, and implementing the law of sines, Eq. (17) is obtained:

$$\overline{OH}_j = \|\mathbf{v}\| \frac{sin\frac{\theta_j}{2}}{sin\,\omega_j} \tag{17}$$

where $\theta_A = \theta_C = \theta_{x'}$ and $\theta_B = \theta_D = \theta_{y'}$.

In this way, Eqs. (18) and (19) are derived. Of course, the sign of the vector components for the four faces follows the position on the *xyz* reference system as in Fig. 5.

$$\mathbf{OS_j} = \left(\frac{\overline{OH}_j}{\cos\rho_j}, 0, 0\right) \tag{18}$$

$$\mathbf{OP_j} = \left(0, \frac{\overline{OH}_j}{\sin\rho_j}, 0\right) \tag{19}$$

Considering the triangle OVS_j, it is obtained that

$$\widehat{VOS_J} = \cos^{-1}\frac{\mathbf{OS_j}\cdot\mathbf{v}}{\|\mathbf{v}\|\|\mathbf{OS_j}\|} \tag{20}$$

Again, by applying the law of sines to triangle OVS_j, it is obtained that

$$\frac{\|\mathbf{v}\|}{\sin\widehat{OS_JV}} = \frac{\|\mathbf{OS_j}\|}{\sin\widehat{OVS_J}} = \frac{\|\mathbf{VS_j}\|}{\sin\widehat{VOS_J}} \tag{21}$$

Given that $\widehat{OS_JV} = 180 - \widehat{OVS_J} - \widehat{VOS_J}$ and with some trigonometric calculations, Eq. (22) is obtained.

$$\sin\widehat{OS_JV} = \sin\left(180 - \widehat{OVS_J} - \widehat{VOS_J}\right) = \sin\widehat{OVS_J}\cos\widehat{VOS_J} + \sin\widehat{VOS_J}\cos\widehat{OVS_J} \tag{22}$$

In this way, combining Eq. (21) and Eq.(22), Eqs. (23)-(25) are obtained:

$$\frac{\|\mathbf{v}\|}{\|\mathbf{OS_j}\|} = \frac{\sin\widehat{OS_JV}}{\sin\widehat{OVS_J}} \tag{23}$$

$$\frac{\|\mathbf{v}\|}{\|\mathbf{OS_j}\|} = \frac{\sin\widehat{OVS_J}\cos\widehat{VOS_J} + \sin\widehat{VOS_J}\cos\widehat{OVS_J}}{\sin\widehat{OVS_J}} \tag{24}$$

$$\frac{\|\mathbf{v}\|}{\|\mathbf{OS_j}\|} = \cos\widehat{VOS_J} + \frac{\sin\widehat{VOS_J}}{\tan\widehat{OVS_J}} \tag{25}$$

and from Eq. (25), Eq. (26) is also obtained:

$$\widehat{OVS_j} = \tan^{-1} \frac{\|\mathbf{OS_j}\| \sin \widehat{VOS_j}}{\|\mathbf{v}\| - \|\mathbf{OS_j}\| \cos \widehat{VOS_j}} \tag{26}$$

By applying the same calculations from Eq. (20) onward to triangle VOP_j, it is found that,

$$\widehat{OVP_j} = \tan^{-1} \frac{\|\mathbf{OP_j}\| \sin \widehat{VOP_j}}{\|\mathbf{v}\| - \|\mathbf{OP_j}\| \cos \widehat{VOP_j}} \tag{27}$$

Therefore, considering a single *j*-th indenter face, the angles between two opposite edges can be found according to:

$$\alpha_j = 2\, \widehat{OVP_j} \tag{28}$$

$$\beta_j = 2\, \widehat{OVS_j} \tag{29}$$

Averaging the results obtained for each *j*-th indenter face, the angles between two opposite edges, nominally 172.5 (Eq. 30) and 130° (Eq. 31), are finally obtained:

$$\alpha = \frac{\sum_{i=1}^{4} \alpha_j}{4} \tag{30}$$

$$\beta = \frac{\sum_{i=1}^{4} \beta_j}{4} \tag{31}$$

4. Comparison of experimental measurements

In order to validate the geometrical model, experimental measurements were performed on three different Knoop indenters previously verified by a German DKD accredited laboratory (MPA NRW DKD-K-06301) having comparable measurement uncertainties. Calibration certificates data with expanded uncertainties at a confidence level of 95 % are reported in Table 1.

Verification of the Knoop indenters' geometrical parameters was performed at INRiM with the Galileo-LTF® Gal-Indent optical system, described in Section 2. Experimental results are reported in Table 2.

In this way, by applying the geometrical model of Section 3, the complete set of experimental values required for the verification of the Knoop indenters are obtained and summarized in Table 3. Expanded uncertainties ($k = 2$, at a confidence level of 95 %), evaluated according to GUM using as input uncertainties of the Vickers diamond indenter angle measurements [8] (CMCs declared in the CIPM-MRA database (KCDB)), are in order of 0.05°, thus below the maximum expanded uncertainty of 0.07° required by the Standard.

Table 1 - Calibration certificate values of the three tested Knoop indenters

	Knoop indenter 1	*Knoop indenter 2*	*Knoop indenter 3*
ID number	3522	3528	3521
Angle between the opposite edges α /°	172.53 ± 0.03	172.50 ± 0.03	172.50 ± 0.03
Angle between the opposite edges β /°	130.13 ± 0.07	129.83 ± 0.07	130.02 ± 0.07
Tilt angle δ /°	<0.42 ± 0.07	<0.42 ± 0.07	<0.42 ± 0.07
Numerical factor c / -	0.07018 ± 0.00030	0.07001 ± 0.00030	0.07031 ± 0.00030

Table 2 - Experimental measurements of the three tested Knoop indenters.

	Knoop indenter 1	*Knoop indenter 2*	*Knoop indenter 3*
ω_A /°	25.146	25.297	25.197
ω_B /°	25.151	25.275	25.184
ω_C /°	25.151	25.310	25.193
ω_D /°	25.152	25.278	25.174
φ_1 /°	165.03	163.86	163.48
τ_1 /°	16.07	16.05	15.43
φ_2 /°	163.01	164.23	164.56
τ_2 /°	15.90	15.86	16.53

Table 3 - Geometrical parameters of the three tested Knoop indenters evaluated with the geometrical model

	Knoop indenter 1	*Knoop indenter 2*	*Knoop indenter 3*
ID number	3522	3528	3521
Angle between the opposite edges α /°	172.53 ± 0.05	172.50 ± 0.05	172.52 ± 0.05
Angle between the opposite edges β /°	130.13 ± 0.05	129.85 ± 0.05	130.06 ± 0.05
Tilt angle δ /°	0.09 ± 0.05	0.03 ± 0.05	0.06 ± 0.05
Numerical factor c / -	0.07019 ± 0.00048	0.07007 ± 0.00047	0.07019 ± 0.00048

An analysis based on the estimation of the normalized error (E_n) has been performed in order to assess the compatibility of the experimental measurements performed at INRiM with respect to calibration certificate values of the accredited laboratory, considered as reference.

From Table 1 and Table 3, it is found that E_n is less than 1 for all geometrical parameters as shown in Table 4. For tilt angle δ, since the calibration certificates report only that the values fall below the limit imposed by the standard, it is not possible to provide the exact normalized error. However, also experimental results show values below the standard limits. Given such evidence, the proposed method provides measurements compatible with the accredited laboratory.

Table 4 - Normalized errors E_n evaluated for the three tested Knoop indenters.

	Knoop indenter 1	*Knoop indenter 2*	*Knoop indenter 3*
Angle between the opposite edges α	0.03	0.06	0.46
Angle between the opposite edges β	0.04	0.19	0.33
Numerical factor c	0.02	0.11	0.21

5. Conclusions

ISO 4545-2 and 4545-3 of Knoop hardness tests require the geometrical verification of the indenter. INRiM hardness laboratory, in cooperation with Galileo-LTF®, developed a specific optical measuring system (commercialized by Galileo-LTF® as Gal-Indent) which is used for the verification of Vickers indenters. This system is also adopted by other NMIs and calibration laboratories around the world. It is able to measure the two vertex angles of the indenter between two opposite faces, and the four angles between two consecutive faces by means of two angular encoders mounted on the optical measuring system. Using such quantities as inputs of the proposed geometrical model described in Section 3, the geometry of Knoop indenters, in particular the angles from the opposite edges at the vertex of Knoop indenters, nominally 172.5° and 130°, and the angle between the axis of the diamond pyramid and the axis of the indenter holder, nominally 0°, can be verified. Experimental measurements, together with the associated expanded uncertainties, were performed on three different Knoop indenters, previously verified by a German DKD accredited laboratory. Comparison of measurement data shows compatible results in terms of normalized error, thus validating the proposed procedure.

References

[1] ISO 4545:2017-2 Metallic materials — Knoop hardness test — Verification and calibration of testing machines.

[2] ISO 4545:2017-3 Metallic materials — Knoop hardness test — Calibration of reference blocks.

[3] Barbato G., Gori G., Metrological references in Hardness Measurement: a necessary background for industrial Quality Assurance, Proceedings of the 5th Congreso Nacional de Metrologia Industrial, Zaragoza, 13-15 November 1991.

[4] Barbato,G., Desogus,S, “Measurement of the spherical tip of Rockwell indenters”, J. of Testing and Evaluation, JTEVA, by the American Society for testing and Materials, vol.16 (4), 1988, p. 369-374.

[5] A. Liguori, A. Germak, G. Gori, E. Messina, Galindent: the reference metrological system for the verification of the geometrical characteristics of Rockwell and Vickers diamond indenters, In: VDI/VDE-GMA, IMEKO TC3/TC5/TC20 Joint International Conference, 24-26 Sept. 2002, VDI-Berichte 1685, Tagung Celle, Germany, 2002, pp. 365-371.

[6] A. Germak, A. Liguori, C. Origlia, Experience in the metrological characterization of primary hardness standard machines, in: Proceedings of HARDMEKO 2007, Tsukuba, Japan, November 19-21, 2007, pp. 81-89.

[7] A. Prato, D. Galliani, C. Origlia, A. Germak, A correction method for Vickers indenters squareness measurement due to the tilt of the pyramid axis, Measurement 140 (2019) 565-571.

[8] JCGM 100:2008, Evaluation of Measurement Data — Guide to the Expression of Uncertainty in Measurement (GUM), Joint Committee for Guides in Metrology, Sèvres, France.